Full length article

# Influence of the composition and viscosity of volcanic ashes on their adhesion within gas turbine aeroengines

J. Dean, C. Taltavull, T.W. Clyne*

Department of Materials Science & Metallurgy, Cambridge University, 27 Charles Babbage Road, Cambridge CB3 0FS, UK

## ARTICLE INFO

## ABSTRACT

This paper presents experimental investigations into adhesion characteristics of four types of (Icelandic) volcanic ash (VA). Firstly, powder (~5—50 μm) was injected into a modified vacuum plasma spray set-up and the fractional mass of particles that adhered to a substrate was measured. Secondly, large (~6 mm), dense pellets of each ash were heated and projected at a substrate, with their impact response monitored via high speed photography. The four ashes fall into two groups of two, one with high Si content (>20%) and the other containing less Si, but higher levels of lower valence cations (such as Ca, Mg & Fe). The glass transition temperatures were all relatively low (~650—750 °C), favouring particle adhesion on surfaces in gas turbines. All of the ashes tended to adhere, especially with higher gas temperatures and impingement velocities. However, this tendency was much greater for the two ashes with high levels of the lower valence cations. The high speed photography confirmed that this was due to these two ashes having much lower viscosities (at high strain rates). This behaviour could not have been predicted solely on the basis of $T_g$ or glass content values. However, these cations act as "network-modifiers" in silica-based glasses, effecting sharp reductions in melt viscosity, so inferences about the danger of specific VA may be possible from simple compositional analysis. In any event, it's clearly important for VA being generated during any particular eruption to be sampled (presumably by drones) and analysed, rather than relying solely on remote measurement of atmospheric ash levels.

## 1. Introduction

Gas turbine aeroengines can be seriously and rapidly damaged by ingested ceramic particles, especially ones that are likely to melt, or at least soften, in flight, and then adhere to solid surfaces on impact. Much ingested particulate has a relatively high softening temperature (>~1300 °C), but this is not the case [1—4] for most types of volcanic ash (VA), which is therefore perceived as particularly dangerous. It's certainly true that a high fraction of ingested particles adhering inside the turbine will lead to serious problems. Even at the VA particle concentration currently classed as "safe" by the CAA (2 mg m$^{-3}$), a large turbofan engine at full power will ingest more than 1 g s$^{-1}$. One gram of adhered particulate, corresponding to ~100 million particles of radius 10 μm, could quickly cause extensive physical damage (blockage of cooling channels etc),

and even much lower levels than this are likely to cause problems such as premature spallation of thermal barrier coatings [5—8].

Of course, there have been increasing levels of concern over the past 20 years about this hazard [9—12], with much attention being devoted to advanced techniques for monitoring concentrations of VA in the atmosphere [13—16]. However, it's clear that not all suspended particulate, and not all types of VA, are equally hazardous. The particle size is one issue, with particles in the range of ~5—50 μm being of most concern - since they are both large enough to give a Stokes number [2,17—19] that ensures frequent impact with solid surfaces and small enough to become substantially heated during passage through the combustion chamber [4]. Unfortunately, particles in this size range are likely both to remain suspended in the air for long periods (partly due to the relatively low density of most volcanic ashes) and also to enter the combustion chamber of an aeroengine [20,21] (rather than being centrifuged into the by-pass air). Furthermore, VAs can vary substantially in composition (depending primarily on the geology of

* Corresponding author.
E-mail address: twc10@cam.ac.uk (T.W. Clyne).

the source area [22,23]) and hence some are likely to be more hazardous than others in terms of their softening temperature and also their viscosity [3,24–29] in the temperature and strain rate ranges of interest, although there is at present very little specific information available in the open literature about this type of property.

The current work involves injection of four different VA powders, comprising particles in this size range of interest, into a set-up designed to simulate passage through a combustion chamber and subsequent projection towards a solid surface. Deposition rates have been measured over a range of conditions. These studies are complemented by high speed photography of pellets (made by sintering the VA powders) after being heated and projected at a substrate.

## 2. Experimental procedures

### 2.1. Powder characterisation

Four ashes have been obtained, from the volcanic eruptions at: (a) Laki (from the fissure eruption of 1783-4 in south-central Iceland), (b) Eldgja (from the fissure eruption of 934, very close to Laki), (c) Hekla 4 - Hekla is a highly active strato-volcano located about 70 km south-west of Laki, which last erupted in 2000 - and (d) Askja 1875 - another active strato-volcano, located about 150 km north-east of Laki, which last erupted in 1961. Papers are available [30–33] covering the details of these eruptions. It's perhaps worth noting at this point that strato-volcanoes, which are characterised by a steep profile, tend to emit highly viscous lava, which cools and hardens before spreading very far [34], although it should be recognised that this is a generalisation and emissions from the same volcano during different eruptions can sometimes vary significantly in composition and viscosity. Such high viscosity also tends to promote high internal pressures, and hence more explosive eruptions [35]. It can thus be seen that an expectation might arise for these four materials to fall into two groups, one comprising ashes (a) and (b) and the other ashes (c) and (d).

The as-received ashes were ground in a ball mill and then passed through a sieve with a mesh spacing of the order of 40 μm. In all cases, this operation produced particle size distributions ranging from about 5 μm to around 50−60 μm. A typical size distribution, referring in that case to the Laki ash, is shown in a previous publication [4]. The chemical compositions of the four ashes, obtained from EDX data, are shown in Fig.1. It can be seen that the concept of there being two groupings is reinforced by this plot, with Laki and Eldgja being similar, as are Hekla and Askja, but with significant differences between the two pairs. The Laki and Eldgja ashes contain only about 15%Si, plus another 20% or so of various other cations, while the Hekla and Askja ashes contain over 20%Si, but less than 15% of the other cations. This is broadly consistent with the concept of material from the Hekla and Askja eruptions being more viscous, since these (low valance) cations are known to act as "network-modifiers" in inorganic glasses, breaking up the linkages between the silica coordination octahedra and hence reducing the viscosity, whereas high silica glasses are expected to be more viscous [36,37]. The higher contents of the divalent (Fe, Ca and Mg) ions in Laki and Eldgja are particularly noticeable.

The phase constitutions of these ashes were investigated using X-ray diffraction. The spectra are shown in Fig.2, together with indications of the phase proportions that they represent. It can be seen that both Hekla and Askja are fully amorphous, while the other two contain significant proportions of two crystalline phases (It was confirmed in a previous publication [4] that most individual particles in the Laki ash are either amorphous or partially crystalline and this is also the case for the Eldgja ash: indexing of the crystalline peaks in Fig.2 is also included in that paper).

A Netzsch dilatometer was used to explore the "softening" behaviour (glass transition temperature and "melting point") of these ashes. Again, details of the procedure used, which involves the actuation rod applying a small pressure to a powder compact while it is heated, are given in the previous paper [4]. The four plots of displacement against temperature (being increased at 5 °C min$^{-1}$) are shown in Fig.3. Initially, the powder compact expands on heating, but then a contraction is observed (on passing through the glass transition temperature, $T_g$), as the amorphous fraction softens, so that powder particles start to deform and the compact becomes denser. For the partially crystalline powders, contraction accelerates when the crystalline phases finally melt at $T_m$. It can be seen from Fig.3 that all of the $T_g$ values are in the approximate range 650−750 °C, while $T_m$ is ~1000−1100 °C for the Laki and Eldgja.
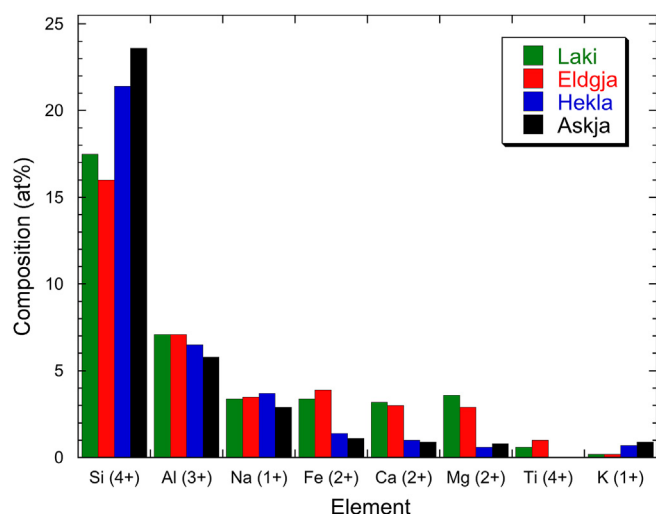
SEM micrographs of the four powders were obtained by



Fig. 1. Compositions of the four ashes, as obtained by EDX (excluding the oxygen content). The expected (predominant) valence states of these cations are indicated.
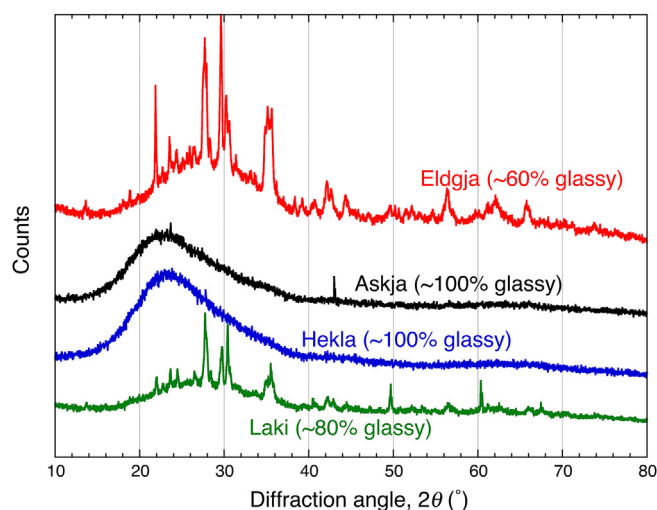


Fig. 2. XRD spectra from the four ashes, with indications of the approximate glass contents (obtained by Rietveldt analysis). The crystalline peaks in the Eldgja and Laki plots are all from two phases, clinopyroxene (~60%) and plagioclase (~40%).
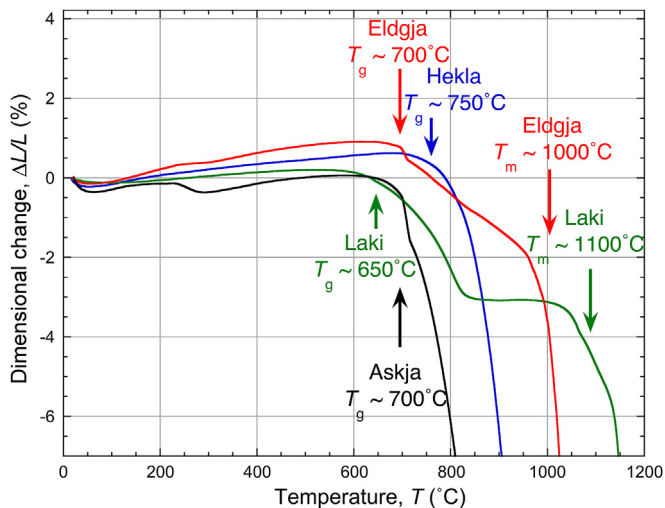
**Fig. 3.** Dilatometry data from the four ashes (as compacted powders), plotted as fractional length change, as a function of temperature (with a heating rate of 5 °C min$^{-1}$). Indications are given in each case of the approximate glass transition temperature and, for the partially crystalline materials, the melting temperature.

sprinkling some particles onto a metallic substrate, followed by sputter coating with gold to prevent charging. A CAMSCAN SEM was used, with a 10 kV accelerating voltage. Representative micrographs are shown in Fig.4. It can be seen that the particles all exhibit rather irregular morphologies. (Of course, these morphologies are not necessarily representative of those exhibited by ash particles in the air after eruptions.)

### 2.2. Particle heating and projection towards a substrate

The factors affecting adhesion of these VA particles were explored using a modified vacuum plasma spray system, in which powder was injected into the front of a plasma torch directed into an open cylindrical tube, at the end of which a substrate was located. The details of this set-up, and of the experimental conditions employed, are presented in the previous publication [4], together with the outcome of CFD modelling work to establish relationships between the operating conditions and the impact velocities and temperatures of individual particles. Three different sets of operating conditions were employed (A, B & C), listed in Table 1 together with corresponding measured temperatures and velocities of the gas and the temperature of the substrate. These experiments all involved stainless steel substrates with a surface finish of 1200 grit, although their temperature and inclination angle were different for different cases. The SEM micrographs in Fig.5 show the appearance of these substrates after such experiments under one of these sets of conditions, for each of the four ashes. It's immediately apparent from these micrographs that Laki and Eldgja particles showed a much greater tendency to adhere to the substrate than did the Hekla and Askja particles, which is consistent with the comments about expected viscosity levels made in the section above, although they all exhibit similar $T_g$ values. These differences in adhesion rates were quantified via measurement of the mass fraction of incident particles that remained attached to the substrates. These results are presented in section 3.

### 2.3. High speed photography of VA pellet impact

While the dilatometry experiments did allow measurement of

the $T_g$ values for the four ashes, further information is required in order to predict the likelihood of different types of ash particle deforming and adhering on impact with solid surfaces. In particular, at least some information is needed about the viscosity (at high strain rates) in the temperature range concerned. This information is not easy to obtain, since most techniques for viscosity measurement do not involve the generation of high strain rates. However, by creating dense spherical pellets of each of the ashes, heating them to appropriate temperatures, projecting them at high velocity towards a substrate, and using high speed photography to record their response, it is at least possible to carry out a ranking exercise with these ashes. (Inferring actual viscosities, or, more accurately, visco-elastic characteristics, should be possible via iterative comparisons between modelled and observed impact responses, using established procedures [38–41], and this is the subject of ongoing work, but is not reported here.)

Pellets were made by placing ash powder in a silicone rubber mould, with the shape of a hollow sphere (8 mm internal diameter and 5 mm wall thickness). This was then cold isostatically pressed, in a Stansted Fluid Power press, with an applied pressure of 1500 bar, for a period of 5 min. The pellets were then removed from the mould and sintered in air for a period of 30 min at 850 °C. Sintering caused a reduction in volume, but the shapes remained spherical. The sintered pellets were fully dense, at least approximately. The diameters after sintering were all around 6.5 mm. Pellets were examined tomographically, using a Skyscan 1172, with a resolution of about 0.5 μm. No pores were detected.

A schematic of the set-up, and also a photograph, are shown in Fig.6. The pellets were located within the barrel of a gas gun, the details of which are supplied elsewhere [42]. For these experiments, the normal steel barrel was replaced by a ceramic tube. The pellet was located within the tube, which contained an inserted graphite sleeve acting as a susceptor that coupled well to the induction field. This field was created using a Cheltenham Induction Heating Ltd system, operating at a frequency of about 140 kHz, with a typical power level of about 0.9 kW. The pellets were heated mainly via radiation from the graphite sleeve. The relationship between induction heating parameters and the thermal history of the pellets was established via experiments in which a thermocouple was located in a small hole drilled into a pellet. This allowed the temperature of the pellets to be pre-programmed for the ballistic experiments (during which thermocouples could not be used).

The high speed photography was carried out using a Phantom camera, details of which are available elsewhere [43]. The frame speed was 9348 fps, the exposure time was 5 μs and the image resolution was 1280 × 536 pixels. A number of experimental runs were carried out. The ejection velocities of the pellets were ~100 m s$^{-1}$, which is of the same approximate magnitude as the impact velocities of the particles during the adhesion experiments [4] - see Table 1.

### 3. VA particle deposition characteristics

The mass fraction of incident particles adhering to the substrates is plotted in Fig.7, as a function of substrate temperature, for all four ashes, and for two substrate inclination angles. As expected, higher substrate temperatures (and the associated higher gas temperatures and velocities) and higher (closer to normal incidence) angles both favour higher rates of adhesion. It was shown in the previous paper [4], using CFD modelling of particle thermal and trajectory histories, that these adhesion rate tend to become substantial as the temperature of the particles in the size range of primary interest (~5–50 μm) start to rise above $T_g$.

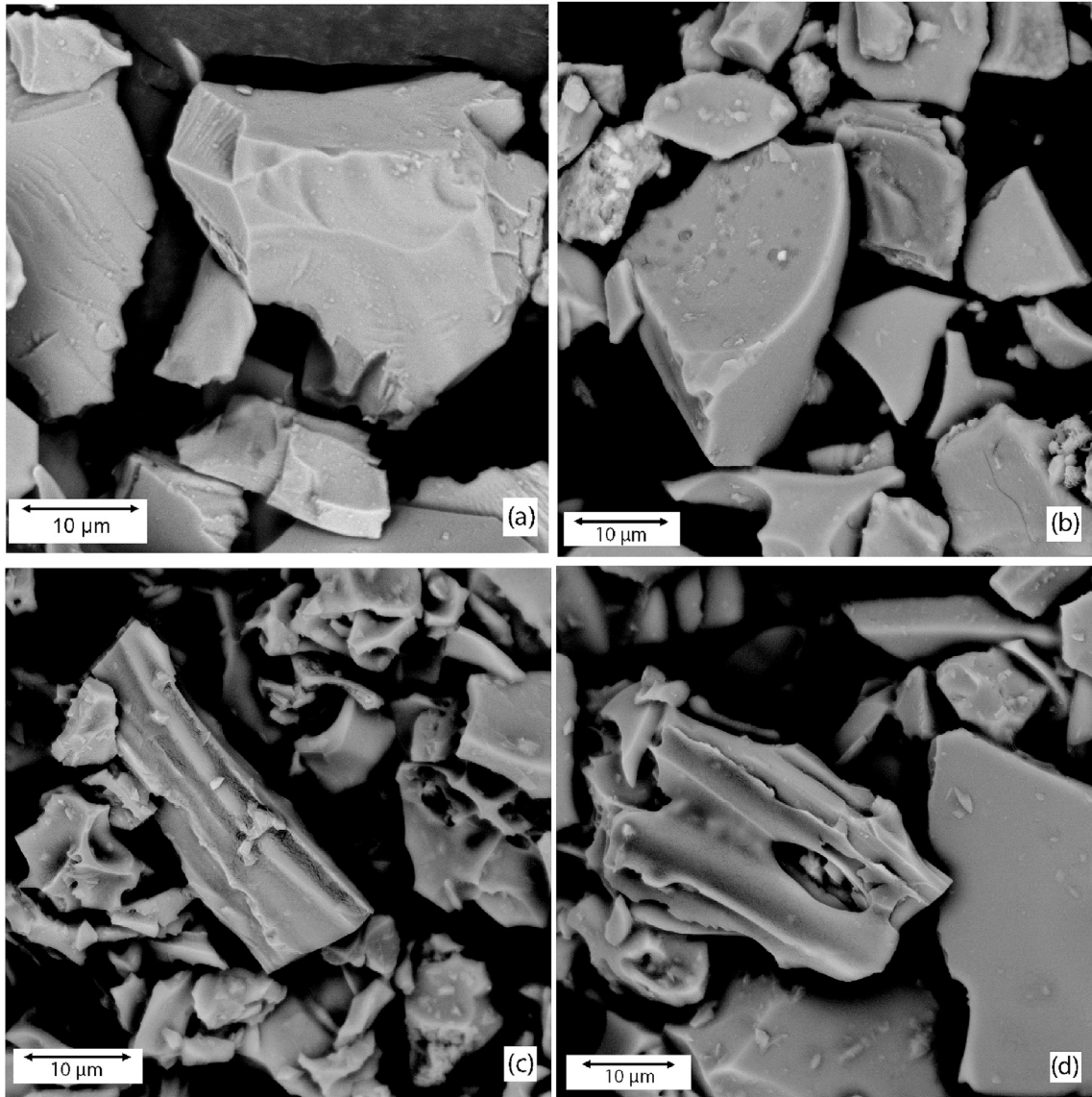This was shown in the previous paper only for the Laki ash, but a

**Fig. 4.** SEM micrographs showing typical particle morphologies for the four types of ash: (a) Laki, (b) Eldgja, (c) Hekla and (d) Askja.

**Table 1**
Sets of operating conditions employed in the tests.

| Case code | Chamber pressure (mbar) | Plasma power (kW) | Temperatures (℃) | | | | | | Speeds (m s$^{-1}$) at x (mm) | |
| | | | Gas at x (mm) | | | Substrate (x = 450 mm) | | | | |
| | | | 175 | 340 | 500 | $\theta = 90°$ | $\theta = 60°$ | $\theta = 30°$ | 350 | 450 |
|---|---|---|---|---|---|---|---|---|---|---|
| A | 120 | 30 | 1115 | 839 | 770 | 410 | 404 | 429 | 92.2 | 90.6 |
| B | 100 | 35 | 1415 | 970 | 885 | 526 | 528 | 560 | 106.8 | 105.9 |
| C | 80 | 40 | 1932 | 1143 | 1022 | 600 | 621 | 659 | 127.5 | 126.9 |

similar outcome also applies to the Eldgja ash. However, it can be seen in Fig.7 that the Hekla and Askja ashes behave rather differently. Although they have similar $T_g$ values (Fig.3), their rates of deposition are noticeably lower. Of course, there is invariably some scatter in the results obtained during this type of experiment, but nevertheless this trend is very clear. The effect is also illustrated by the micrographs shown in Fig.5, which relate to a case for which all of the deposition rates are relatively low, but those of Laki and Eldgja are clearly higher than those for the Hekla and Askja (see

Fig.7). That this is related to differences in the viscosity of these two different types of ash (in the high strain rate regime that is relevant to impact deformation) is confirmed by the high speed photography results presented in the next section.

## 4. VA pellet impact behaviour

Figs. 8–11 show sets of video stills for the four ashes. In all of these cases, the initial pellet temperature was about 1200 °C. It may
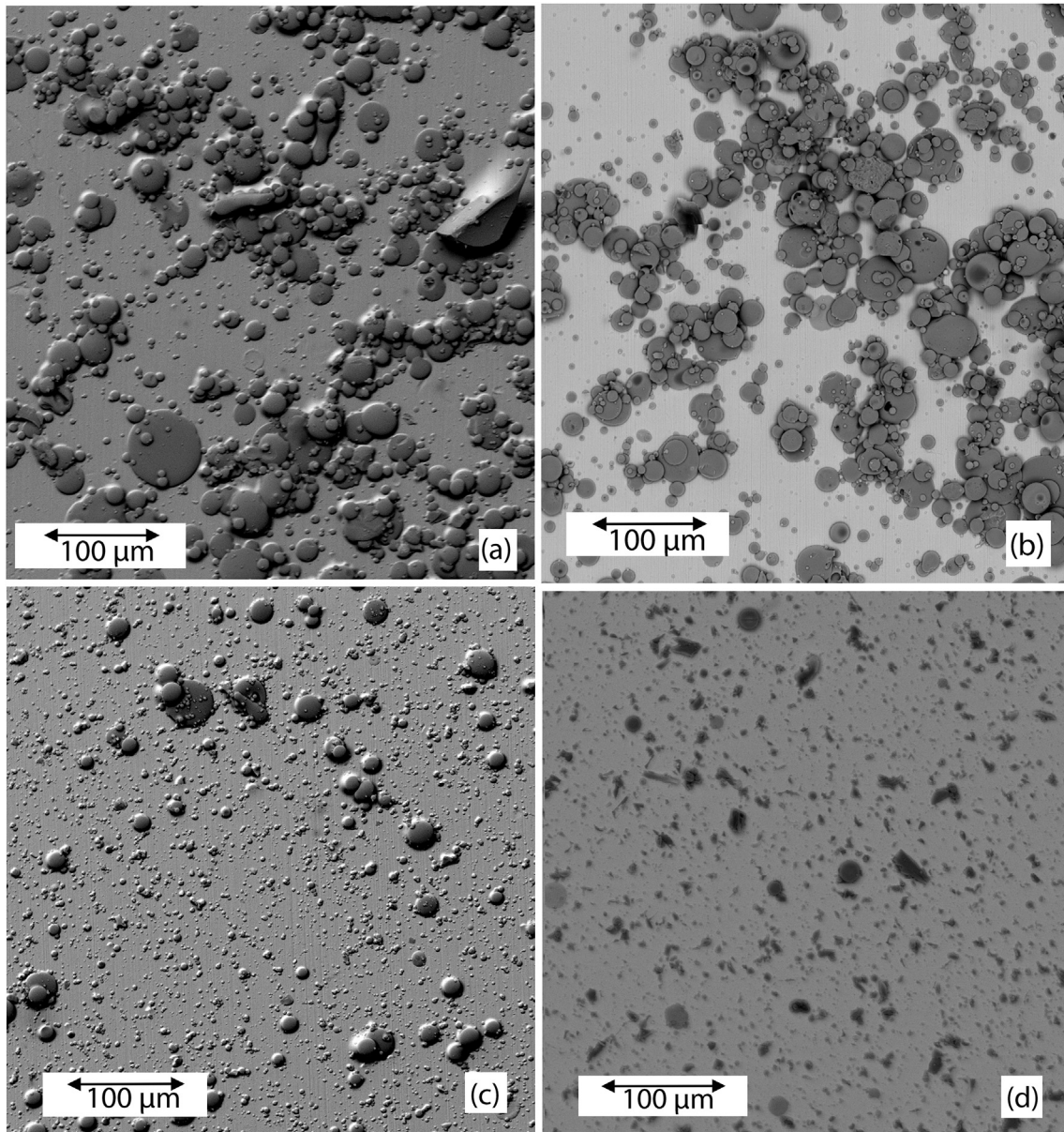
**Fig. 5.** SEM micrographs of substrates, under condition A, with normal incidence (see Table 1), after injection of the four types of ash: (a) Laki, (b) Eldgja, (c) Hekla and (d) Askja.

be noted that this is above the $T_g$ and $T_m$ values in all cases, so these pellets are nominally expected to be liquids. In practice, they are liquids with relatively high viscosity (even under quasi-static conditions), so that they all remained at least approximately spherical while in the bore of the gas gun. However, it can be seen from these figures that the behaviour exhibited by the Laki and Eldgja pellets (Figs. 8 and 9) was noticeably different from that of the other pair (Figs. 10 and 11). In the former case, the pellets clearly broke up in flight and deformed substantially on impact. (None of these pellets or fragments actually adhered to the substrate, which is unsurprising in view of their large size, and also in view of the fact that the substrate was cold.) The Hekla and Askja pellets on the other hand, largely retained their spherical shape in flight and rebounded from the substrate in what appear to be largely elastic events, although some fracture did occur with the Hekla pellet. This is clearly an indication of a substantially higher viscosity (at these

very high strain rates) for these two ashes, compared with that of the Laki and Eldgja. Of course, this is consistent with the behaviour exhibited by the powder particles, with the Hekla and Askja ashes exhibiting noticeably lower rates of adhesion. (The particle temperatures were somewhat lower in those experiments, but it seems reasonable to expect that these differences in viscosity between the two pairs of materials would be exhibited across a range of temperature.)

## 5. Conclusions

The following conclusions can be drawn from this work.

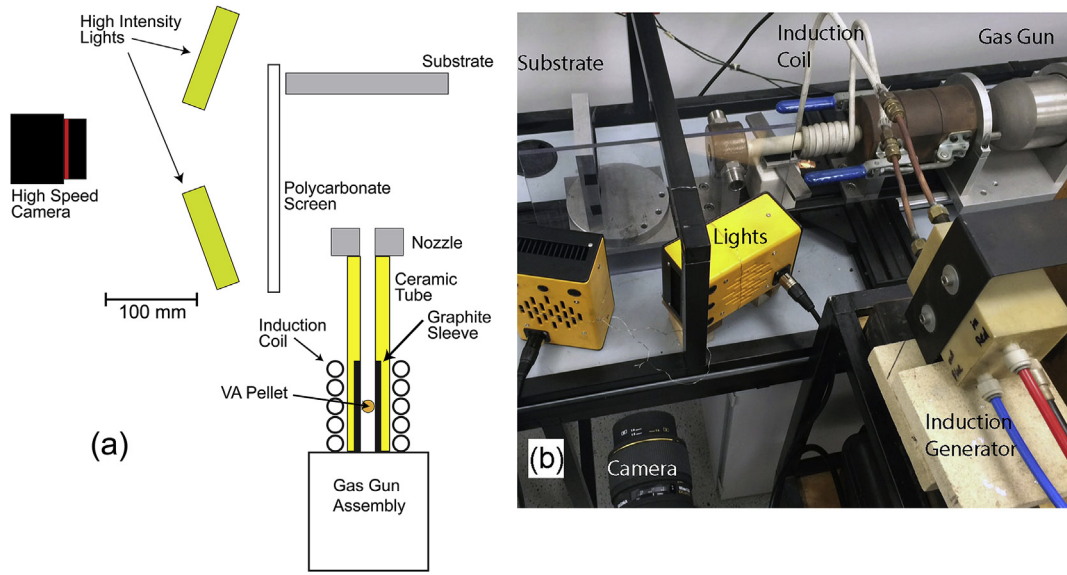(a) Four ashes have been examined and these can be divided into two groups, one pair from typical strato-volcanoes

**Fig. 6.** (a) Schematic plan view and (b) photo of the gas gun and high speed photography set-up.
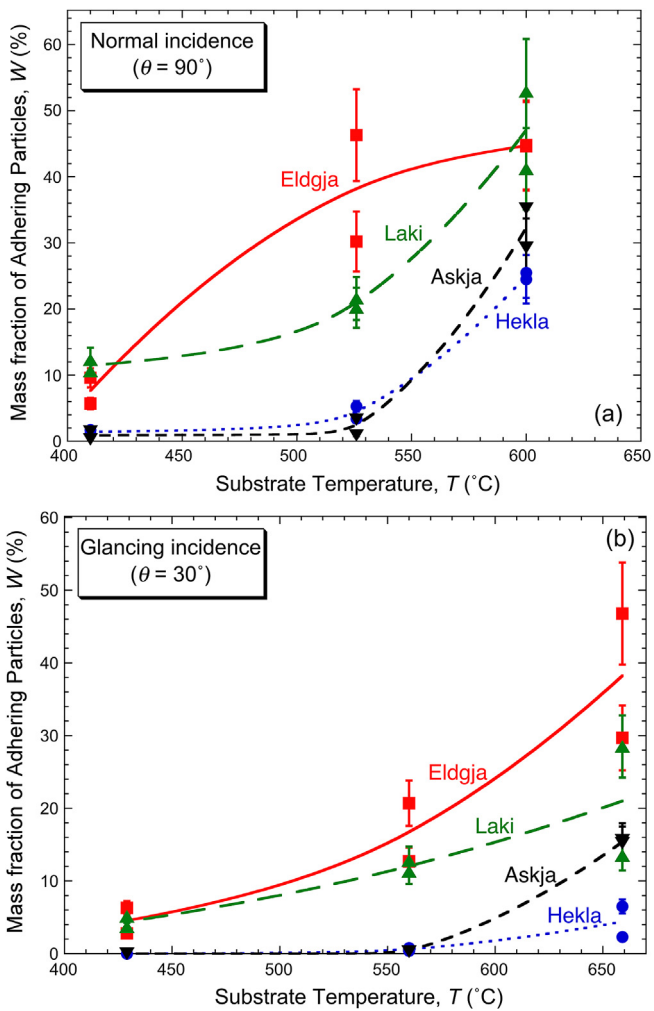


**Fig. 7.** Particle adhesion data for the four ashes, showing the mass fraction of projected particles adhering to the substrate, as a function of the substrate temperature (reflecting the severity of the thermal and velocity fields), for angles between the incident particle trajectory and the substrate surface of (a) 90° and (b) 30°.
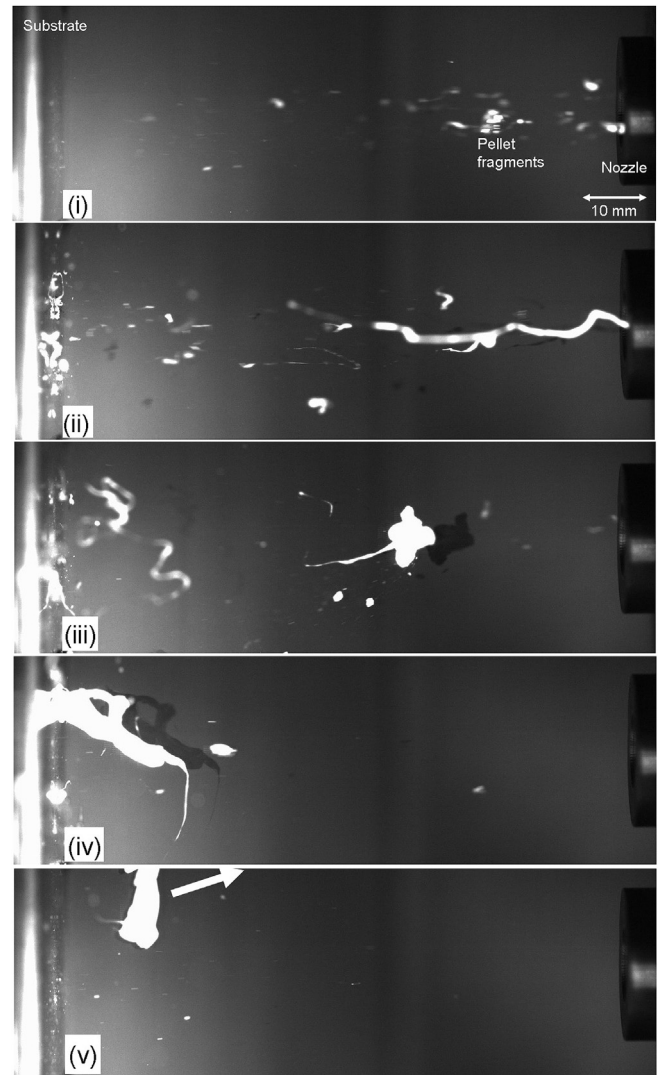


**Fig. 8.** Series of video stills for projection of a Laki pellet, with an initial temperature of 1200 °C, corresponding to times of (i) 0.75 ms, (ii) 1.60 ms, (iii) 2.46 ms, (iv) 3.21 ms and (v) 5.35 ms.
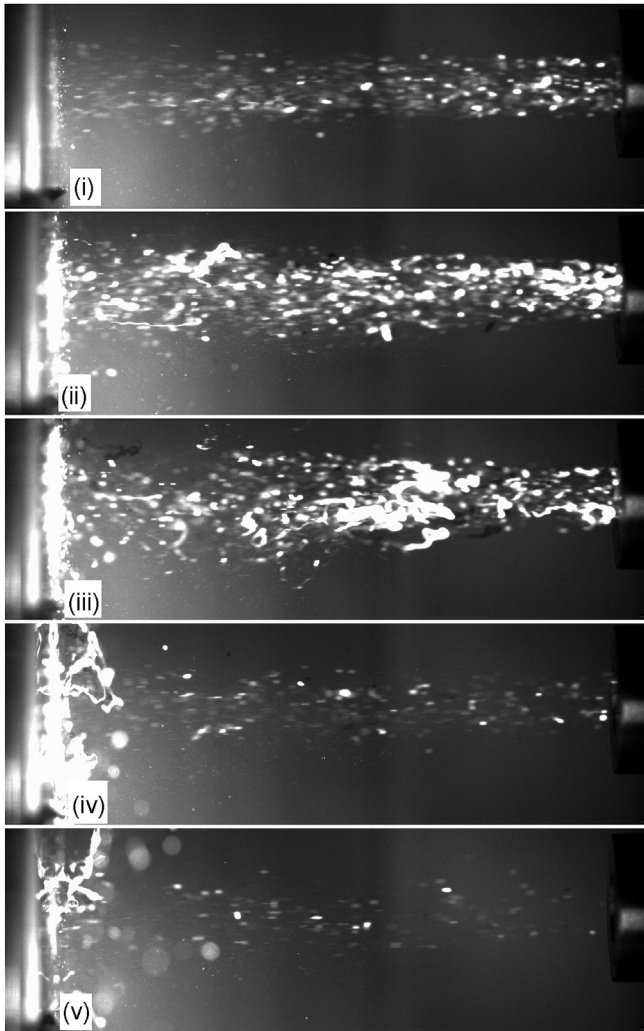
**Fig. 9.** Series of video stills for projection of an Eldgja pellet, with an initial temperature of 1200 °C, corresponding to times of (i) 1.07 ms, (ii) 2.03 ms, (iii) 2.89 ms, (iv) 4.28 ms and (v) 5.78 ms.
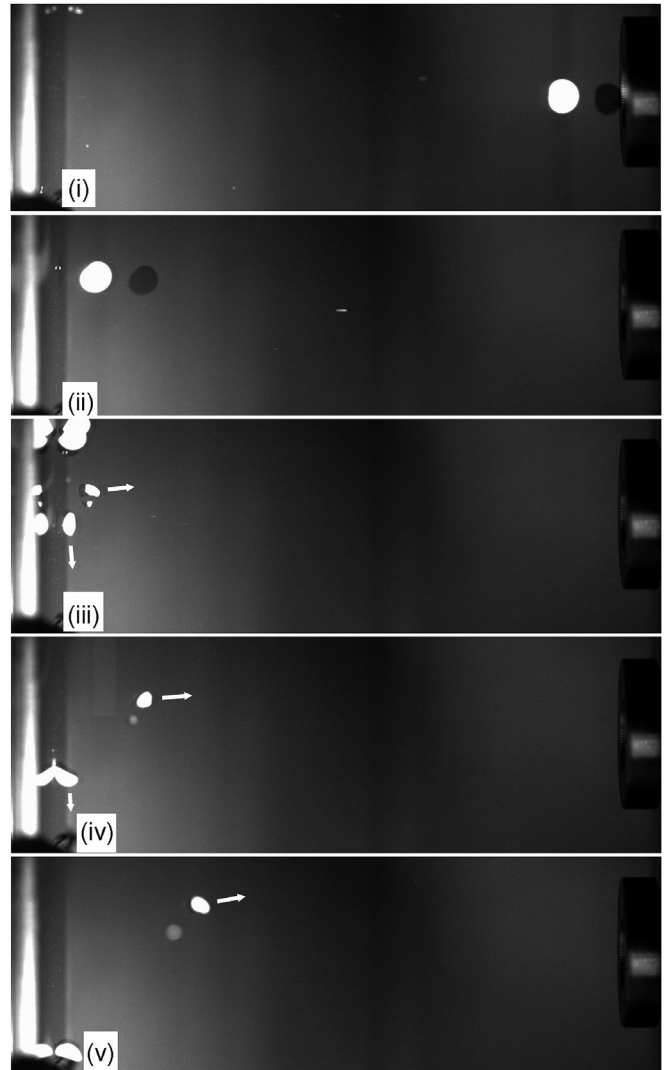


**Fig. 10.** Series of video stills for projection of a Hekla pellet, with an initial temperature of 1200 °C, corresponding to times of (i) 1.39 ms, (ii) 2.46 ms, (iii) 3.21 ms, (iv) 4.07 ms and (v) 5.03 ms.

(Hekla and Askja), which are expected to have relatively high viscosities, and the other two (Laki and Eldgja) from a region characterised by extensive fissures and fluid near-surface magma. The compositions of Laki and Eldgja are relatively high in cations such as $Ca^{2+}$, $Fe^{2+}$ and $Mg^{2+}$, which are likely to act as "network-modifiers" in these glasses and hence reduce the viscosity. The other two ashes are silica-rich and contain lower levels of such cations. These compositions are therefore consistent with expectations based on the type of volcano from which they were obtained.

(b) While all of the ash types exhibited greater rates of particle adhesion in hotter gas streams, and for higher angles of incidence to the substrate, these rates were noticeably lower for the two ashes with the high silica content. This suggests that, in addition to $T_g$ being significant, the viscosity of the material (at the temperature concerned, and at high strain rate) can affect the likelihood of adhesion, and may be sensitive to ash composition.

(c) Relatively large, fully dense pellets of the four ashes were projected, at high velocity and high temperature, towards a cold substrate, with in-flight and impact behaviour being monitored by high speed photography. In these experiments as well, clear differences were observed between the two groups, with the high silica ashes behaving in a visco-elastic manner indicative of a high viscosity, while the other two types of pellet responded much more like conventional liquids, breaking up in flight and undergoing extensive deformation on impact with the substrate.

(d) In view of the observed sensitivity to composition, and consequent differences in (high strain rate) viscosity and hence in the likelihood of adhesion within gas turbines, it seems advisable for particulate volcanic emissions to be characterised in this way, in addition to particle size distribution. Evidently, (remote) monitoring of atmospheric levels of ash is insufficient. Fortunately, obtaining such samples (presumably via drones) and making such measurements (of PSD and composition) should be straightforward. These findings are apparently novel and further work is needed, particularly on the significance of (high strain rate) viscosity and the nature of the linkages to composition.
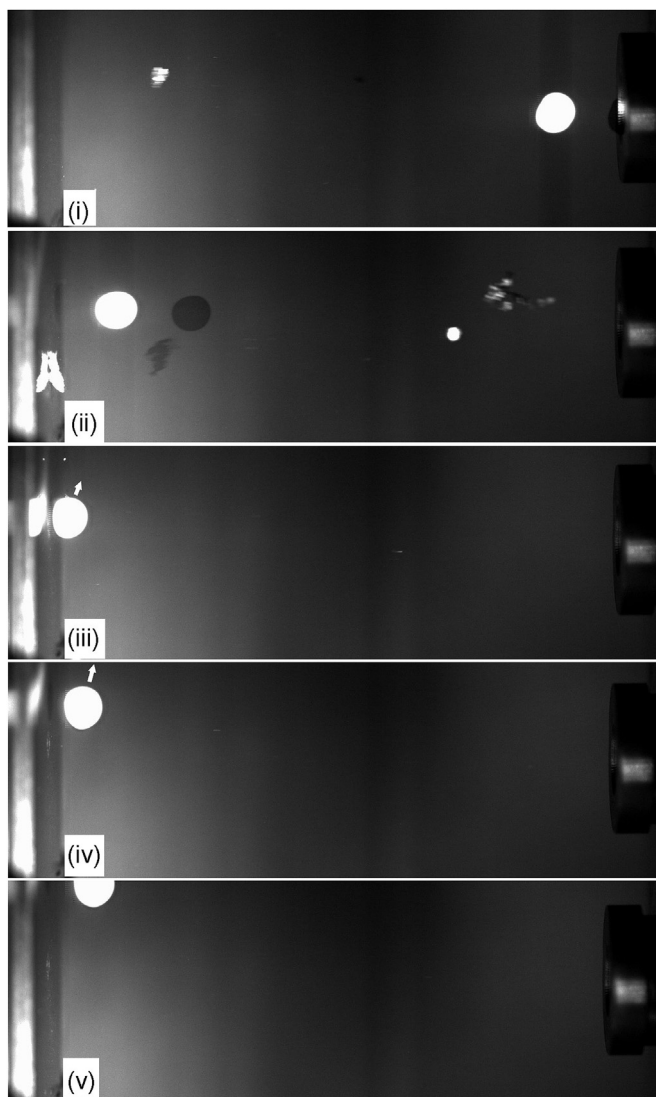
**Fig. 11.** Series of video stills for projection of an Askja pellet, with an initial temperature of 1200 °C, corresponding to times of (i) 1.60 ms, (ii) 2.25 ms, (iii) 2.89 ms, (iv) 3.96 ms and (v) 5.35 ms.

## Acknowledgements

## References

[1] J. Kim, M.G. Dunn, A.J. Baran, D.P. Wade, E.L. Tremba, Deposition of volcanic materials in the hot sections of 2 gas-turbine engines, J. Eng. Gas Turbines Power-Trans. ASME 115 (3) (1993) 641–651.

[2] M. Shinozaki, K.A. Roberts, B. van de Goor, T.W. Clyne, Deposition of ingested volcanic ash on surfaces in the turbine of a small jet engine, Adv. Eng. Mater. 15 (10) (2013) 986–994.

[3] W.J. Song, K.U. Hess, D.E. Damby, F.B. Wadsworth, Y. Lavallee, C. Cimarelli, D.B. Dingwell, Fusion characteristics of volcanic ash relevant to aviation hazards, Geophys. Res. Lett. 41 (7) (2014) 2326–2333.

[4] C. Taltavull, J. Dean, T.W. Clyne, Adhesion of volcanic ash particles under controlled conditions and implications for their deposition in gas turbines, Adv. Eng. Mater. (2016), http://dx.doi.org/10.1002/adem.201500371.

[5] J.M. Drexler, A.D. Gledhill, K. Shinoda, A.L. Vasiliev, K.M. Reddy, S. Sampath, N.P. Padture, Jet engine coatings for resisting volcanic ash damage, Adv. Mater. 23 (21) (2011) 2419–2424.

[6] M. Shinozaki, T.W. Clyne, The effect of vermiculite on the degradation and spallation of plasma sprayed thermal barrier coatings, Surf. Coatings Technol. 216 (2013) 172–177.

[7] U. Schulz, W. Braue, Degradation of La2Zr2O7 and other novel EB-PVD thermal barrier coatings by CIVIAS (CaO-MgO-Al2O3-SiO2) and volcanic ash deposits, Surf. Coatings Technol. 235 (2013) 165–173.

[8] K.I. Lee, L.T. Wu, R.T. Wu, P. Xiao, Mechanisms and mitigation of volcanic ash attack on yttria stabilized zirconia thermal barrier coatings, Surf. Coatings Technol. 260 (2014) 68–72.

[9] M.G. Dunn, A.J. Baran, J. Miatech, Operation of gas turbine engines in volcanic ash clouds, J. Eng. Gas Turbines Power-Trans. Asme 118 (4) (1996) 724–731.

[10] C. Witham, H. Webster, M. Hort, A. Jones, D. Thomson, Modelling concentrations of volcanic ash encountered by aircraft in past eruptions, Atmos. Environ. 48 (2012) 219–229.

[11] M.G. Dunn, Operation of gas turbine engines in an environment contaminated with volcanic ash, J. Turbomachinery-Trans. Asme (5) (2012) 134.

[12] C.R. Davison, T.A. Rutke, Assessment and characterization of volcanic ash threat to gas turbine engine performance, J. Eng. Gas Turbines Power-Trans. Asme (8) (2014) 136.

[13] N. Pergola, V. Tramutoli, F. Marchese, I. Scaffidi, T. Lacava, Improving volcanic ash cloud detection by a robust satellite technique, Remote Sens. Environ. 90 (1) (2004) 1–22.

[14] G. Gangale, A.J. Prata, L. Clarisse, The infrared spectral signature of volcanic ash determined from high-spectral resolution satellite measurements, Remote Sens. Environ. 114 (2) (2010) 414–425.

[15] T. Steensen, P. Webley, Ieee, Qualitative analysis of input parameters for satellite-based quantification of airborne volcanic ash, in: 2012 Ieee International Geoscience and Remote Sensing Symposium, Ieee, New York, 2012, pp. 2982–2985.

[16] S. Mackie, M. Watson, Atmospheric dependency of the sensitivity of infrared satellite observations to volcanic ash clouds, J. Appl. Remote Sens. (2015) 9.

[17] M. Kostoglou, A.G. Konstandopoulos, Particulate deposit shape evolution on cylinders in cross-flow at high Stokes numbers, J. Aerosol Sci. 31 (4) (2000) 427–436.

[18] N.E.L. Haugen, S. Kragset, Particle impaction on a cylinder in a crossflow as function of Stokes and Reynolds numbers, J. Fluid Mech. 661 (2010) 239–261.

[19] C. Bonilla, J. Webb, C. Clum, B. Casaday, E. Brewer, J.P. Bons, The effect of particle size and film cooling on nozzle guide vane deposition, J. Eng. Gas Turbines Power-Trans. Asme (10) (2012) 134.

[20] W. Tabakoff, A. Hamed, M. Metwally, Effect of particle-size distribution on particle dynamics and blade erosion in axial-flow turbines, J. Eng. Gas Turbines Power-Trans. Asme 113 (4) (1991) 607–615.

[21] M.M. Weaver, M.G. Dunn, T. Heffernan, Experimental determination of the influence of foreign particle ingestion on the behavior of hot section components including lamilloy, in: 41st ASME Gas Turbine and Aeroengine Congress, ASME, Birmingham, UK, 1996.

[22] L.M. Larsen, J.G. Fitton, A.K. Pedersen, Paleogene volcanic ash layers in the Danish Basin: compositions and source areas in the North Atlantic Igneous Province, Lithos 71 (1) (2003) 47–80.

[23] H.E. Taylor, F.E. Lichte, Chemical composition of mount St-Helens volcanic ash, Geophys. Res. Lett. 7 (11) (1980) 949–952.

[24] I. Vicentemingarro, J.M. Rincon, P. Bowles, R.D. Rawlings, P.S. Rogers, Viscosity measurements on glasses obtained from alkaline volcanic-rocks of the Canary-Islands, Glass Technol. 33 (2) (1992) 49–52.

[25] J. Gottsmann, D. Giordano, D.B. Dingwell, Predicting shear viscosity during volcanic processes at the glass transition: a calorimetric calibration, Earth Planet. Sci. Lett. 198 (3–4) (2002) 417–427.

[26] D. Giordano, M. Potuzak, C. Romano, D.B. Dingwell, M. Nowak, Viscosity and glass transition temperature of hydrous melts in the system CaAl2Si2O8-CaMgSi2O6, Chem. Geol. 256 (3–4) (2008) 203–215.

[27] D. Giordano, J.K. Russell, D.B. Dingwell, Viscosity of magmatic liquids: A model, Earth Planet. Sci. Lett. 271 (1–4) (2008) 123–134.

[28] M. Hobiger, I. Sonder, R. Buttner, B. Zimanowski, Viscosity characteristics of selected volcanic rock melts, J. Volcanol. Geotherm. Res. 200 (1–2) (2011) 27–34.

[29] F.B. Wadsworth, J. Vasseur, F.W. von Aulock, K.U. Hess, B. Scheu, Y. Lavallee, D.B. Dingwell, Nonisothermal viscous sintering of volcanic ash, J. Geophys. Research-Solid Earth 119 (12) (2014) 8792–8804.

[30] T. Thordarson, S. Self, The Laki (Skaftar-fires) and grimsvotn eruptions in 1783-1785, Bull. Volcanol. 55 (4) (1993) 233–263.

[31] T. Thordarson, D.J. Miller, G. Larsen, S. Self, H. Sigurdsson, New estimates of sulfur degassing and atmospheric mass-loading by the 934 AD Eldgja eruption, Iceland, J. Volcanol. Geotherm. Res. 108 (1–4) (2001) 33–54.

[32] A. Gudmundsson, N. Oskarsson, K. Gronvold, K. Saemundsson, O. Sigurdsson, R. Stefansson, S.R. Gislason, P. Einarsson, B. Brandsdottir, G. Larsen, H. Johannesson, T. Thordarson, The 1991 eruption of Hekla, Iceland, Bull. Volcanol. 54 (3) (1992) 238–246.

[33] H. Sigurdsson, R.S.J. Sparks, Petrology of rhyolitic and mixed magma ejecta from the 1875 eruption of Askja, Iceland, J. Petrol. 22 (1) (1981) 41–84.

[34] S.A. Fagents, T.K.P. Gregg, R.M.C. Lopes, Modeling Volcanic Processes: the Physics and Mathematics of Volcanism, Cambridge University Press, , Cambridge, 2013.

[35] H.M. Gonnermann, M. Manga, The Fluid Mechanics inside a Volcano, Ann. Rev. Fluid Mech. 39 (2007) 321–356.

[36] F. Branda, A. Buri, D. Caferra, A. Marotta, The effect of mixing of network-modifiers on the transformation temperature of silicate-glasses, J. Non-Crystal. Solids 54 (1–2) (1983) 193–198.

[37] J.F. Stebbins, J.V. Oglesby, Z. Xu, Disorder among network-modifier cations in silicate glasses: New constraints from triple-quantum O-17 NMR, Am. Mineral. 82 (11–12) (1997) 1116–1124.

[38] G. Trapaga, E.F. Matthys, J.J. Valencia, J. Szekely, Fluid-flow, heat-transfer, and solidification of molten-metal droplets impinging on substrates - comparison of numerical and experimental results, Metall. Trans. B-Process Metall. 23 (6) (1992) 701–718.

[39] Z. Zhao, D. Poulikakos, J. Fukai, Heat transfer and fluid dynamics during the collision of a liquid droplet on a substrate .1. Modeling, Int. J. Heat Mass Transf. 39 (13) (1996) 2771–2789.

[40] H. Tabbara, S. Gu, Numerical study of semi-molten droplet impingement, Appl. Phys. A Mater. Sci. Process. 104 (4) (2011) 1011–1019.

[41] C. Le Bot, S. Vincent, E. Meillot, F. Sarret, J.P. Caltagirone, L. Bianchi, Numerical simulation of several impacting ceramic droplets with liquid/solid phase change, Surf. Coatings Technol. 268 (2015) 272–277.

[42] J. Dean, C.S. Dunleavy, P.M. Brown, T.W. Clyne, Energy absorption during projectile perforation of thin steel plates and the kinetic energy of ejected fragments, Int. J. Impact Eng. 36 (10–11) (2009) 1250–1258.

[43] S.C. Troughton, A. Nomine, A.V. Nomine, G. Henrion, T.W. Clyne, Synchronised electrical monitoring and high speed video of bubble growth associated with individual discharges during plasma electrolytic oxidation, Appl. Surf. Sci. 359 (2015) 405–411.